ON THE ASSIMILATION OF Ku-BAND SCATTEROMETER WINDS FOR WEATHER ANALYSIS AND FORECASTING

J. Figa* , A. Stoffelen

KNMI Postbus 201, 3730 De Bilt, The Netherlands

Phone: +31 30 220 6585, Fax: +31 30 221 0843

e-mail: figa@knmi.nl, stoffelen@knmi.nl

(*) Present affiliation:
EUMETSAT, Postfach 10 05 55. D-64205 Darmstadt. Phone: +49 6151 807455, Fax: +49 6151 807838, e-mail: figa@eumetsat.de

ABSTRACT

Following the successful assimilation of ERS scatterometer winds for weather analysis and forecasting, we further develop this methodology for the assimilation of NSCAT and QuikSCAT Ku-band scatterometer data. Besides retrieval problems in cases of a confused sea state, the Quality Control developed here identifies cases with rain on a WVC (Wind Vector Cell) by WVC basis. The elimination of such geophysical conditions is a prerequisite to arrive at a successful assimilation of Ku-band scatterometer data. Moreover, we propose to assimilate ambiguous winds rather than radar backscatter measurements, as is being done at most meteorological centres assimilating ERS scatterometer data. After our quality assessment, NSCAT winds still have more difficult ambiguity removal properties than ERS winds. A further testing of the data assimilation method proposed is being carried out at ECMWF in NSCAT impact experiments.

A normalised wind inversion residual is used for Quality Control. In order to determine a threshold for the rejection of poor quality wind solutions, the inversion residual and the wind vector departure from the ECMWF model are correlated. We end up rejecting around 7.4 % of wind vector solutions and 4.2% of the NSCAT WVCs. In order to perform a qualitative assessment of this rejection, comparisons to collocated SSM/I rain and ECMWF winds are used. Confused sea state and presence of rain seem to be the most likely causes for the rejection of WVCs. As expected, the remaining number of ambiguities is larger than in the case of the ERS scatterometer, but dependent on wind direction. The proposed cost function for the assimilation of NSCAT winds in weather analysis contains up to four ambiguous winds, the derived quality control information and the probability of each wind solution. We believe that the results of our study can be successfully extended for the interpretation and retrieval of good quality winds from QuikSCAT and their assimilation in weather analysis.

Keywords: scatterometer, wind, quality control, inversion, cost function, rain, 4D variational numerical prediction model.

I. INTRODUCTION

The forecast of extreme weather events is not always satisfactory, while its consequences can have large human and economic impact. The lack of data over the oceans, where many weather disturbances develop, is one of the main obstacles to Numerical Weather Prediction (NWP) models in predicting their intensity and position. A space-borne scatterometer is able to provide accurate

winds over the ocean surface and can potentially contribute to improve the situation for tropical and extratropical cyclone prediction [1] [2].

NSCAT, the National Astronautics and Space Administration (NASA) scatterometer, operated on the Advanced Earth Observing Satellite (ADEOS) for nine months (September 1996 – June 1997). It featured three fan beams with varying azimuth angle and polarisation, which illuminated a 600-km wide swath on the ocean surface on both sides of the spacecraft. Within the swath the backscatter measurements were binned in areas of size 50kmX50km, called Wind Vector Cell or WVC [3]. QuikSCAT, the present NASA scatterometer, was launched in summer 1999. In order to have an operational product to be assimilated in weather analysis, the information content of QuikSCAT winds has to be assessed. QuikSCAT is a Ku-band scatterometer as was NSCAT, and consequently has very similar Quality Control (QC) issues to review, such as the effects of the presence of rain on the wind quality. Moreover, although the viewing geometry and polarisation coverage are generally different between NSCAT and QuikSCAT, similar wind direction ambiguity problems are present for most of the QuikSCAT swath [4]. The general objective of this work is to prepare for QuikSCAT data QC and assimilation, by assessing the information content of the winds retrieved from the NSCAT scatterometer. This is particularly important in order to assimilate QuikSCAT data in weather analysis as soon as they become available.

Lacking other estimation of the quality of scatterometer wind data, the RMS (Root Mean Square) wind vector difference with respect to the weather model (background) winds provides an effective QC in many cases. However, in cases where the background wind is grossly in error, a wrong scatterometer wind ambiguity that confirms the model state may be selected, and the true ambiguity may be lost. Obviously, it is precisely in the cases where the background model state is grossly in error that we would like the observations to correct it. Therefore, an important requirement for the effective assimilation of data into weather analysis is to have an assessment of their accuracy independent from the model state itself. With that purpose, we look into the retrieval process of scatterometer winds in order to determine what quality information is available. In case of NSCAT, we measure usually four independent quantities, i.e., the fore, mid and aft beam vertical polarisation backscatter (VV), and the mid beam horizontal polarisation backscatter (HH). From these four measurements we retrieve two geophysical quantities, i.e., wind speed and wind direction, and information on the wind retrieval performance.

The retrieval is an inversion problem for each WVC that, given a set of measurements σ^o_{oi}, finds the wind vector (V,ϕ) that according to the Geophysical Model Function (GMF) has the highest probability of representing the true wind. An inversion problem presented in these probabilistic terms is usually equivalent to the minimisation of a cost function J (also called Maximum Likelihood Estimator or MLE) (see for example [5]), which in case of the NSCAT wind retrieval has the following expression:

$$J(V,\phi) = \sum_{i=1}^{N} \left[\frac{\sigma^o_{oi} - \sigma^o_{si}(V,\phi)}{SD(\sigma^o_{si}(V,\phi))} \right]^2$$

[Eq.1]

where σ^o_{si} is the backscatter associated with different trial values of (V,ϕ) through the GMF, $SD(\sigma^o_{si})$ is its corresponding standard deviation and N is the number of measurements within the WVC (for a size of the WVC of 50x50 km, N can be up to 24, but is typically 16 [6]). J indicates therefore how well the backscatter measurements used in the retrieval of a particular wind vector fit the GMF, and gives therefore a good indication about the quality (interpretability) of that measurement. Often, when assuming Gaussian errors, an additional term $\sum\{\ln[SD(\sigma^o_{si})]^2\}$ is added

to the previous expression of J [7]. However, we have verified that its contribution is mostly constant and does not affect the wind retrieval significantly. Therefore we did not use it for our study. One assumption in the formulation of the problem is related to the GMF, which is empirically determined for fair weather conditions, i.e. average sea state and generally in the absence of rain, for which conditions a satisfactory wind-backscatter relationship has been established [8]. The specification of the noise of the system in $SD(\sigma^o_{si})$ is important in this respect. The noise is assumed to be Gaussian in σ^o and can be attributed to three different sources:

a) the instrument noise,
b) the measurement collocation error due to the variability of the wind within the WVC, and
c) the uncertainty in the GMF.

For those geophysical conditions where the GMF is poorly known, we would prefer to assign poor quality to the retrieved wind vector. This could be done by not accounting for the GMF error in $SD(\sigma^o_{si})$ and then using J as a quality indicator. The retrieved wind would then be the most probable wind, assuming a perfect GMF. However, wind inversion is not the subject of this paper, but quality assessment. The wind inversion that formed the basis of our study has either been provided by JPL [6], or been produced at KNMI by simulating the JPL inversion, and in any case is based on the assumptions about the GMF and the noise explained above. We verified that the results are not sensitive to the precise inversion formula used (see e.g. figure 1). QC and inversion problems can thus be investigated separately.

For this study, we use the most up-to-date GMF's (NSCAT-1 [8] and NSCAT-2). NSCAT data from the JPL PODAAC (Physical Oceanography Distributed Active Archive Center) were used [6]. Collocations with operational ECMWF (European Centre for Medium-range Weather Forecasts) FGAT winds (First Guess at Appropriate Time) [9] and with SSM/I rain measurements from the NASA Pathfinder data set are used to assess the performance of the QC method.

II. METHOD PROPOSED

The best QC indicator appears in principle to be J. However, figure 1 shows that, when using the $SD(\sigma^o_{si})$ as specified in the first NSCAT products, J is strongly dependent on wind speed and swath position (squares). However, the quality of the retrieved wind shows less variability with wind speed and swath position according to NSCAT wind validation (see e.g. [10]). Therefore, this J is not useful for quality assessment of NSCAT wind retrievals before their assimilation in weather analysis, since the accuracy and information content of certain wind speeds and swath positions would systematically be wrongly assessed. In order to better reflect the true noise properties of the winds, we have normalised J as a function of wind speed and swath position by its expected value J^*, which we compute as follows:

$$J^*(V,\phi) = \sum_{i=1}^{N} \left[\frac{SD^*(\sigma^o_{si}(V,\phi))}{SD(\sigma^o_{si}(V,\phi))} \right]^2 \qquad \text{[Eq.2.1]}$$

$$SD^*(\sigma^o_{si}) = \left\langle (\sigma^o_{oi} - \sigma^o_{si}(V,\phi))^2 \right\rangle^{1/2} = \sqrt{SD^2_{INSTRUMENT}(\sigma^o_{si}) + SD^2_{COLLOCATION}(\sigma^o_{si})} \qquad \text{[Eq.2.2]}$$

where $SD^*(\sigma^o_{si})$ represents the expected difference between the observation and the GMF. By using the rightmost expression of Eq. 2.2, we have estimated SD^* as measurement noise, considering the different contributions discussed in section 1. For the instrument noise we have used measurements over arctic sea ice where the target is believed to be uniform and stable over a NSCAT WVC. [11]

provides the estimated instrument error as a function of the backscastter over ice. We have calculated the collocation error using the GMF, after estimating from a climate spectrum a wind speed variability within the 50-km WVC of 0.5 ms^{-1}, independent of wind direction [12]. As in [9], it is assumed that due to surface friction the 10m wind has 75% of the general variability present in the lower troposphere. This error variance contribution to the total error mainly affects the normalisation for medium to low wind speeds and is dominant over the instrument error for low wind speeds. The contribution of the GMF uncertainty has not been included in *SD**, since in case of large GMF error, anomalous geophysical conditions due to confused sea state or rain are usually present for which the GMF and thus the wind retrieval is invalid. Our aim is to reject such wind retrievals. Measurements in exceptional geophysical conditions should be detected by our new QC indicator (normalised inversion residual), which we formulate as:

$$R_n = SQRT\left(\frac{J}{J^*}\right)$$

[Eq.3]

Figure 1 shows how *J** successfully normalises *J* (triangles) and that R_n is basically independent of wind speed and swath position, and is in this respect a good candidate for the QC of NSCAT winds with generally uniform quality for all WVCs and wind speeds. Note that our error model (estimate of *SD**) is based on instrument properties and geophysical noise due to imperfect collocation of the backscatter footprints, and that figure 1 validates that this error model works to remove WVC and speed dependencies.

III. RESULTS

A. Comparison to the ECMWF-model RMS wind vector difference

For every WVC, up to four wind solutions that provide the lowest minima of *J* have been retrieved using NSCAT-2 and the inversion defined above, and their corresponding R_n values have been calculated. Because of the symmetry of the problem, implicit in the formulation of the GMF, we find in most of the cases those four solutions aligned in two pairs. Within each pair, the two solutions show comparable wind speed and R_n, but a wind direction that differs by 180^o. We denote the pair with the lowest R_n the 'main ambiguous solutions', which generally represent a solution close to the 'true' wind and its 180^o ambiguity. The RMS wind vector difference between ECMWF and NSCAT of this 180^o ambiguity depends on the wind speed. Particularly in cases of average to high wind speeds, this value is generally very high and cannot be usefully related to the quality of the solution as estimated after the inversion (and shown by R_n). Therefore, we have carried out our comparison by taking into account only the solutions within 90^o of the ECMWF wind vector. After this selection, about 50% of the solutions are left, indicating that the solution pattern is indeed symmetric. Figure 2 shows a clear correlation between ECMWF-RMS and R_n, up to R_n values of 4, which supports the use of R_n as an indicator of the information content of the retrieved solutions. 99.7 % of the solutions have R_n values lower than 4, and the 'branches' at the right side of the plot (0.3 % of the solutions) appear at certain wind directions relative to the satellite track (see also figure 5b), and are related to the geometry of the measurement system.

B. The selection of a R_n threshold for rejection of poor retrievals

R_n=4 is the most loose threshold to pick in order to accept solutions from the point of view of interpretability. However, by looking more closely at several situations where bad wind retrievals appear, specially those associated to rain episodes, we decided to take a threshold of R_n=1.8 for the

rejection of bad solutions. By lowering the R_n threshold from 4 to 1.8, we reject just a few more solutions with an average ECMWF-RMS of 10.3 ms^{-1}, too high to contribute with meaningful information to the weather analysis, which has an accuracy of about 1 ms^{-1} [12]. A value of R_n=1.8 accepts solutions with an average ECMWF-RMS of 4.2 ms^{-1}. For reference, the operational implementation of a similar QC method in the case of ERS scatterometer data [13], accepts solutions of approximately 3 ms^{-1} ECMWF-RMS for R_n=3.2. In the case of NSCAT, 92.6% of the solutions are accepted and 7.4% rejected, the latter with a high average ECMWF-RMS of 10.6 ms^{-1}, which again supports the effectiveness of the threshold chosen. The number of WVCs with one or more solution accepted is 96.8%.

After the rejection of solutions, there is a small number of WVCs which are accepted but where one of the two main ambiguous solutions is rejected and only one solution is left or occasionally more than one but separated by less than 90^o. In those cases the accepted solution(s) is just below the threshold and the rejected one(s) just above. Apparently, there is an anomalous geophysical condition, since no solutions well below the threshold exist, and in fact there is a major risk that the solution representing the true wind vector is rejected. In the absence of the true solution there is obviously no point in keeping the other solutions and attempting to use these in the ambiguity removal step following the inversion. Therefore, we have decided to discard these WVCs as well. After this, we are rejecting in total 4.2% of the WVCs. This is more than in the case of the ERS processing at KNMI or ECMWF, but quite acceptable. The results are summarised in tables 1 and 2.

C. Verification of the detection of rain contamination

Collocations between the retrieved winds and SSM/I rain data from the NASA Pathfinder data set [14] were made within 0.25 deg. and 30 minutes. Out of all the solutions considered in figure 2, those collocated with a SSM/I rain event above 12 mm/hr have been plotted in figure 3. It is shown that most of these are rejected by R_n=1.8 and correspond to high ECMWF-RMS values. Very few points appear over the black part of the histogram of figure 2, which corresponds to good quality winds, both according to ECMWF-RMS and to R_n values. As such, our quality control appears to effectively reject rain-contaminated retrievals. In next section we investigate the spatial characteristics of the scheme.

D. Some cases for illustration

We have looked at several particular cases to check how the QC performs. Figures 4a and 4b show two typical NSCAT passes where the QC has been applied. Erroneous solutions along and across the satellite track appear, but our QC rejects these and only accepts both main ambiguous solutions. The success of this rejection is better in the mid to inner swath, while in the outer swath all solutions are accepted in most of the cases.

Figure 4c shows a likely case of undeveloped sea state (see for example [15]) in a coastal area (Alaska), where the wind blows offshore with great force. This is a special sea state that does not correspond to the general weather conditions for which the GMF has been derived [8]. Many spurious solutions appear in the area, which are rejected by the QC. At a certain distance from the coast, the sea has developed into an equilibrium state with the local surface wind and the rejections disappear. The reason why the rejection occurs so far away from the coast is probably related to the presence of coastal sea ice, since the measurements correspond to high latitudes in winter.

Figure 4d shows a case of tropical rain, where the GMF sensitivity to wind appears to be anomalous. This figure suggests that the area where the poor solutions appear matches in general the area where rain has been detected by SSM/I. However, the identification of rain-contaminated solutions from SSM/I collocations only, does not seem to correspond always on a WVC by WVC

basis with the QC, and some WVCs are rejected by the QC but do not contain much rain according to the SSM/I rain product. This is not surprising, since intense rain cells in tropical areas tend to be very localised (within an area of very few kilometers), and SSM/I is not able to detect them if they do not fill a significant part of the beam footprint. This points out the difficulty of developing a rain flag based only on rain observations from SSM/I.

Figure 4e shows a case of rain outside the tropics. As expected, low rain rates do not affect the retrieval significantly. In this case the rejected WVCs may correspond to the confused sea state (see e.g. [16] for the effect of wind direction variation on sea state) associated with the edge of the front, where a few poor retrievals are rejected. We have found that rejections appear systematically in this type of situations, as has also been our experience with the ERS scatterometer QC.

In figure 4f a situation is shown which illustrates the slight increase in the average R_n value for the inner swath suggested in figure 1 (lower panel). In many cases a few spurious solutions appear systematically in the inner WVCs. They commonly correspond to high wind speeds (above 15 ms^{-1}), as is also suggested by the curve slope towards higher wind speeds in figure 1 (upper panel). If we include in figure 1 (lower panel) solutions with wind speeds above 15 ms^{-1}, the increase of R_n for the inner WVCs is accentuated (plot not shown). We think that this problem has to do with the NSCAT-2 GMF and the formulation of J (Eq. 1), which might perform less well for the inner WVCs at high wind speeds. Fortunately, our QC properly rejects these wrong solutions.

E. The wind direction dependency of $\boldsymbol{R_n}$ and ECMWF-RMS

Although R_n is basically independent of wind speed or swath position, figure 5 indicates that the inversion performance is wind direction dependent, as is the ECMWF-RMS. That dependency has symmetry with respect to the satellite track, and is therefore related to the geometry of the measurement system. In figure 5a it is shown that many solutions along and, to a lesser extent, perpendicular to the ground track exist with a large deviation from ECMWF. The main reason is not that wind directions of the true solution retrieved along these directions are less accurate than those for other directions. This was verified by a scatter plot similar to figure 5a, but only for the solution closest to ECMWF. In that case the contour lines are much more circular (not shown). However, we have noted that the wind directions along and across the ground track direction occur more frequently as ambiguous solution. In Figure 4a one can see examples of ambiguous along-track solutions, as well as a few in figure 4b. Figure 4e shows some across-track ambiguities south of the front. The occurrence of these solutions depends on the NSCAT antenna geometry and the retrieval cost function (Eq. 1). We are investigating whether a small modification of the cost function changes the character of the ambiguities [17].

IV. THE ASSIMILATION OF NSCAT WINDS IN ATMOSPHERIC MODELS

A 4D variational scheme such as the ECMWF NWP model consists of the minimisation of a cost function $\Im$, i.e.,

$$\Im = \Im_O + \Im_B + \Im_C \qquad \text{[Eq.4]}$$

where $\Im_O$ represents the differences between the control variables and the observations, $\Im_B$ represents the differences between the control variables and the background field and $\Im_C$ is a small term expressing physical constraints on the atmospheric state.

Following Stoffelen and Anderson [9], the observational error of each of the individual scatterometer ambiguities in a wind WVC can be characterised by a normal distribution in the wind components. Using the available ambiguities, a $\Im_O^{NSCAT}$ can be built in the wind domain for each NSCAT wind WVC, representing the information content and uncertainties of the set of backscatter measurements and is expressed as a weighted sum of each individual solution as follows:

$$\Im_O^{NSCAT} = -2\ln\left\{\sum_{i=1,N} \boldsymbol{N}(V_i, e_i)P_i\right\}$$

[Eq.5]

where N is the number of up to four scatterometer wind ambiguities (V_i) and e_i describes the width of the normal distribution $\boldsymbol{N}$, according to the accuracy of that particular wind solution. P_i expresses the probability of each solution.

As shown in section 3, the normalised inversion residual R_n is a good indicator of the quality of each scatterometer wind solution. R_n therefore contributes in defining both e_i and P_i. From figure 2, table 1, and under the condition where we accept solutions with R_n less than 1.8, we heuristically propose an expression for e_i:

$$e_i = 1 + 0.5R_{ni}{}^2$$

[Eq.6]

The probability P_i of each solution is expressed as follows:

$$P_i = \frac{P_i^r P_i^d}{\sum_{j=1,N}(P_j^r P_j^d)}$$

[Eq.7]

P^d_i is an *a priori* probability of wind direction. Without any prior information about the wind direction quality of each of the ambiguous solutions, not all of them have the same probability of being correct, and P^d_i is related to the angular sector which that particular solution represents, as shown in figure 6.

$$P_i^d = \frac{\gamma_i}{2\pi}$$

[Eq.8]

P^r_i contains the probability of the solution after wind retrieval and is a function of R_n. From our statistics we heuristically derived the following expression:

$$P_i^r = \mathrm{Max}(1 - 0.2\mathrm{R}_{ni}^2, 0)$$

[Eq.9]

providing high probability for small residuals and zero probability for $R_n > \sqrt{5}$. Note that the QC derived in the previous section is implied in the definition of $\Im_O^{NSCAT}$, where for Rn > 1.8 a small probability remains (< 33%). As an illustration, figure 7a shows $\Im_O^{NSCAT}$ for one NSCAT wind WVC. The probability distribution is plotted as a function of the wind components and reflects a typical situation of four symmetric solutions including the main ambiguous solutions. For comparison, we also plot in figure 7b the NSCAT inversion residual J from Eq.1.

We note that using the inversion residual in 4D-var (i.e., replacing $\Im_O^{NSCAT}$ in Eq. 5 with a term similar to J) is consistent with specifying a cost function in σ^o instead of a cost function for the retrieved winds. It corresponds to assuming that the main uncertainty of the problem can be specified in the radar backscatter measurement domain as a normally distributed error, in contradiction to [18, 12]. Note in 7b the steep cost gradient for low wind speed, the relatively smooth gradient for high wind speed, and the weak gradients as a function of wind direction. The 4D-var scheme follows the maximum gradient for the minimisation of $\Im$. Regardless of the background, if we choose to specify a σ^o cost function instead of a wind function, the very steep gradient of J around low wind speeds is bound to dominate the total $\Im$ gradient and low wind speeds would seldom be chosen as the solution, resulting in a bias. On the other extreme, background values of very high wind speed would converge very slowly to a lower scatterometer speed solution. Furthermore, in case that the background differs slightly from a particular solution, the analysis would draw to the solution wind speed more than to the solution wind direction, as the former provides a larger gradient generally. In practise, however, there are no indications of an anisotropy in the wind vector determination (accuracy) around the true solution; deviations to high or low wind speeds, or into the lateral or transverse wind component directions appear equally likely. As the plot in figure 7a shows, $\Im_O^{NSCAT}$ presents such symmetric properties, and the problems with anisotropic gradients are circumvented if the cost function is specified in the wind domain as in [18]. The NSCAT cost function proposed here is being tested in the ECMWF 4D-var data assimilation system.

V. CONCLUSIONS AND FUTURE WORK

Following developments in the interpretation and assimilation of ERS scatterometer winds in NWP, we extended this methodology to Ku-band NSCAT data. A normalised residual R_n is derived from the expected error characteristics of the NSCAT scatterometer and provides a uniform cost as a function of wind speed and swath position. It is a good quality indicator for the NSCAT winds and therefore can provide useful additional information for their assimilation.

We find that R_n=1.8 is a very reasonable threshold for rejection of poor retrievals, and in many cases it rejects indeed solutions affected by anomalous geophysical conditions not modelled by the GMF, such as confused sea state or rain. In the particular case of rain, we believe that rejection by the R_n threshold value is probably more appropriate than a WVC –by WVC rain flag from SSM/I collocated rain information. Furthermore, this may be the only viable approach for the real-time application of Ku-band scatterometer data, due to the tight spatial and temporal collocation constraint for rain data.

An open issue which remains, is to investigate the wind direction dependency of R_n, which we believe is related to the definition of J [5]. The radar backscatter depends in a non-linear way on the wind direction (harmonic) and the transformation of the backscatter observation noise through the inversion problem may give rise to systematic errors that depend on wind direction. This is reflected in the behaviour of R_n as a function of wind direction. We note here that the number of acceptable wind solutions depends on wind direction and wind speed, but also on the definition of J, which makes the selection of the most optimal J a difficult (non-linear) task.

A cost function $\Im_O^{NSCAT}$ for the assimilation of NSCAT winds in weather analysis has been proposed using up to four ambiguous solutions and the results of the inversion QC. The shape of $\Im_O^{NSCAT}$ presents more symmetric properties than the normalised inversion residual, and shows the advantage of assimilating winds vs. σ^o's in a 4D variational data assimilation scheme. At the

moment of writing this paper, an impact study on the assimilation of NSCAT winds in weather analysis is ongoing in co-operation with ECMWF in order to test the definition of $\Im_O^{NSCAT}$.

After the impact study of NSCAT winds on NWP, the objective is to apply the same methodology to QuikSCAT. QuikSCAT is the first of a new generation of Ku-band scatterometers, based on a scanning pencil-beam concept, as opposed to the fixed antenna geometry of fan-beam scatterometers such as ERS, NSCAT or ASCAT. In most of the swath, a wind retrieval similar to NSCAT or ERS can be applied and we plan to implement similar processing to that described here. In the far and nadir areas of the QuikSCAT swath, some more development will be necessary, since there we lack polarisation or azimuth look coverage and will have a less well-determined wind vector, which suggests the use of a more complex inversion, QC, and data assimilation approach.

REFERENCES

[1] L. Isaksen, D. Le Meur, A. Stoffelen., Impact of ERS scatterometer wind data on ECMWF's analyses and forecasts of tropical cyclones. *Proceedings of the ESA workshop on Scatterometer Applications, from research to operations,* pp.177-183, 1998.

[2] A. Stoffelen & P. van Beukering. Implementation of improved ERS scatterometer data processing and its impact on HIRLAM short range weather forecasts. Report for the Beleidscomissie Remote Sensing, contract NRSP-2/97-06, 1997.

[3] F. M. Naderi, M. H. Freilich, and D. G. Long, Spaceborne radar measurement of wind velocity over the ocean – An overview of the NSCAT scatterometer system, *Proc. IEEE 79*, 850-866, 1991.

[4] T.E. Oliphant and D. Long, Accuracy of scatterometer-derived winds using the Cramér-Rao Bound. *IEEE Transaction on Geoscience and Remote Sensing*, vol. 37, NO. 6, pp 2642-2652, 1999.

[5] A.Stoffelen & D.Anderson. Scatterometer data interpretation: Measurement space and inversion. *Journal of Atmospheric and Oceanic Technology*, vol.14, pp.1298-1313, 1997.

[6] NASA Scatterometer Science Data Product User's Manual, Version 1.1, April 1997, JPL PODAAC, Pasadena, California, USA; http://jpl.noaa.gov/podaac.

[7] W.J. Pierson, Probabilities and statistics for backscatter estimates obtained by a scatterometer, *Journal of Geophysical Research*, vol. 94, NO. C7, pp 9743-9759, 1989.

[8] F.J. Wentz & D.K. Smith. A model function for the ocean normalised cross section at 14 GHz derived from NSCAT observations. *Journal of Geophysical Research,* Special issue on NSCAT: Scientific Applications, vol 104, NO. C5, pp 11,499-11,514, 1999.

[9] A. Stoffelen, Scatterometry, PhD thesis, Utrecht University, the Netherlands, ISBN 90-393-1708-9.

[10] N. Ebuchi, Statistical distribution of wind speeds and directions globally observed by NSCAT, *Journal of Geophysical Research 104* (C5), 11,393-11,403, 1999.

[11] A.Cavanié & R.Ezraty. Evaluation of Kp on central and lateral antennas of NSCAT over Arctic sea ice, *Proceedings of the NSCAT Science Symposium,* pp70-72, NSCAT project, JPL, Pasadena, California, 1997.

[12] D. K. Lilley and E. L. Petersen, Aircraft measurements of atmospheric kinetic energy spectra, Tellus, Ser. A, 35, 379-382, 1983.

[13] A. Stoffelen & D. Anderson, Scatterometer data interpretation: Estimation and validation of the transfer function CMOD4. *Journal of Geophysical Research*, vol. 102(C3), pp. 5767-5780, 1997.

[14] F.J. Wentz & R.W. Spencer, SSM/I rain retrievals within a unified all-weather ocean algorithm. Submitted for *Journal of Atmospheric Sciences*, PIP-2 issue, Feb. 1996.

[15] M. A. Donelan, W. M. Drennan, and K. B. Katsaros, The air-sea momentum flux in conditions of wind sea and swell, *J. Phys. Oceanography 27*, 2087-2099, 1997.

[16] P.A. Hwang, and O.H. Shemdin, The dependence of sea surface slope on atmospheric stability and swell conditions, *Journal of Geophysical Research 93* (C11), 13,903-13,912, 1988.

[17] J. Figa & A. Stoffelen. Towars an improved Ku-band scatterometer wind product. Final report of the NSCAT EUMETSAT Fellowship 97/98, 1999.

[18] A.Stoffelen & D.Anderson. Ambiguity removal and assimilation of scatterometer data. *Quart. J. Royal Meteorological Society 123*, 491-518, 1997.

ACKNOWLEDGEMENTS

This work has been carried out under the EUMETSAT NSCAT fellowship at KNMI. The SSM/I data was retrieved from the Remote Sensing Systems web page. The NSCAT data was downloaded from the PODAAC server at JPL. The three anonymous reviewers provided constructive and relevant comments that improved the readability of the paper considerably.

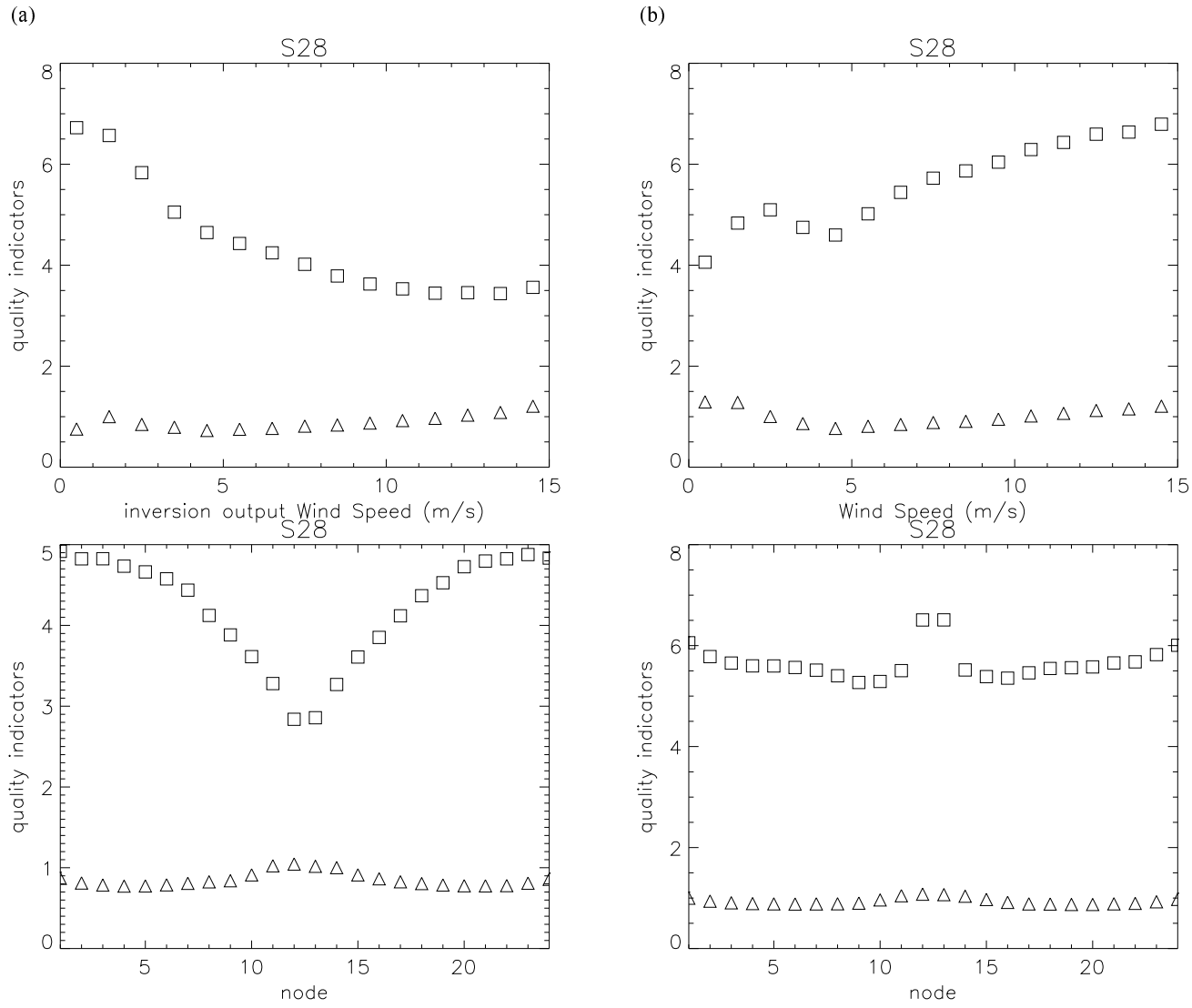

Figure 1. Averaged SQRT(J) (squares) and R_n=SQRT(J/J) (triangles) with respect to wind speed (up) and swath position (low). The data used correspond to five days of data (batch S28) in March. In (a), the 1997 processed σ^o's and NSCAT-1 GMF are used, while in (b) we use the latest processed σ^o's and NSCAT-2. One can see that the situation after the reprocessing improved, since both the wind speed and the WVC dependency of J are less pronounced. Our method normalises J in both cases.*

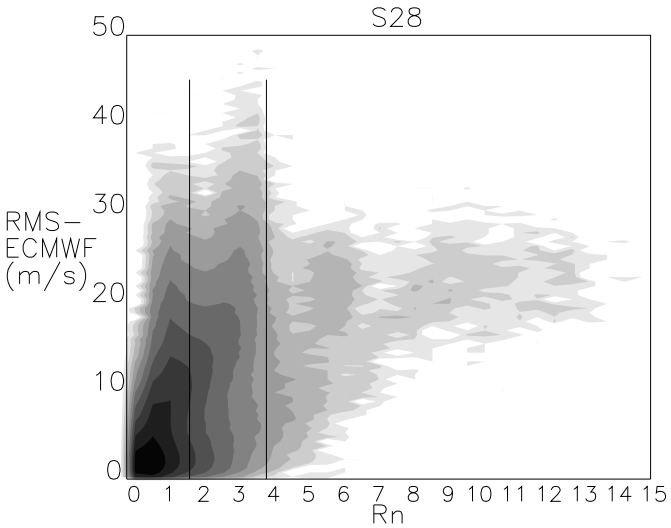

Figure 2. Log-density scatter histogram of (R_n .vs. ECMWF-RMS) points corresponding to wind solutions retrieved from batch S28. The darker areas show where the distribution of points is higher. In the white area no points were found. The grey scale is not linear, but logarithmic, in order to emphasise the distribution shape around the areas were higher values are found. The two vertical lines correspond to R_n=1.8 and R_n=4.0.

WIND SOLUTIONS		avg. ECMWF-RMS
accepted	92.6 %	4.2
rejected	7.4 %	10.6

Table 1. QC statistics in percentage of solutions and average RMSM-ECMWF, after applying a threshold of R_n=1.8 for rejection to batch S28 data (approximately 1,000,000 solutions or five days of data).

WIND WVCS		
accepted	96.8 %	
rejected	3.2 %	
post-rejected	1.0 %	Total rejected: 4.2 %

Table 2. QC statistics in percentage of WVCs, after applying a threshold of R_n=1.8 for rejection of solutions to batch S28 data.

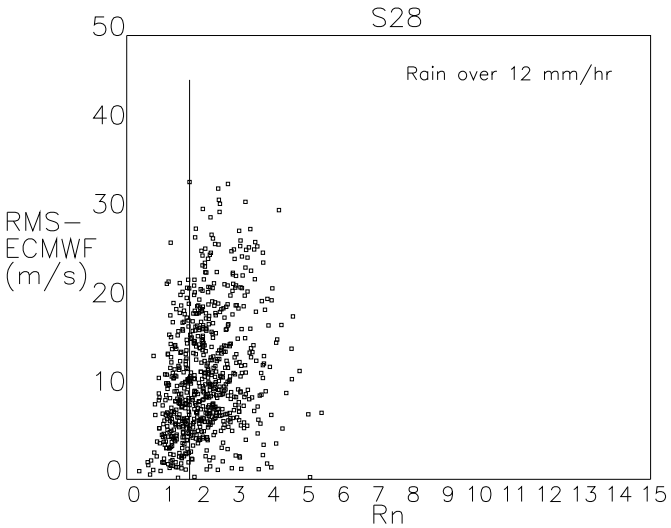

Figure 3. (R_n .vs. ECMWF-RMS) points corresponding to wind solutions retrieved from batch S28 where a SSM/I rain collocation above 12mm/hr has been found. The vertical line corresponds to R_n=1.8

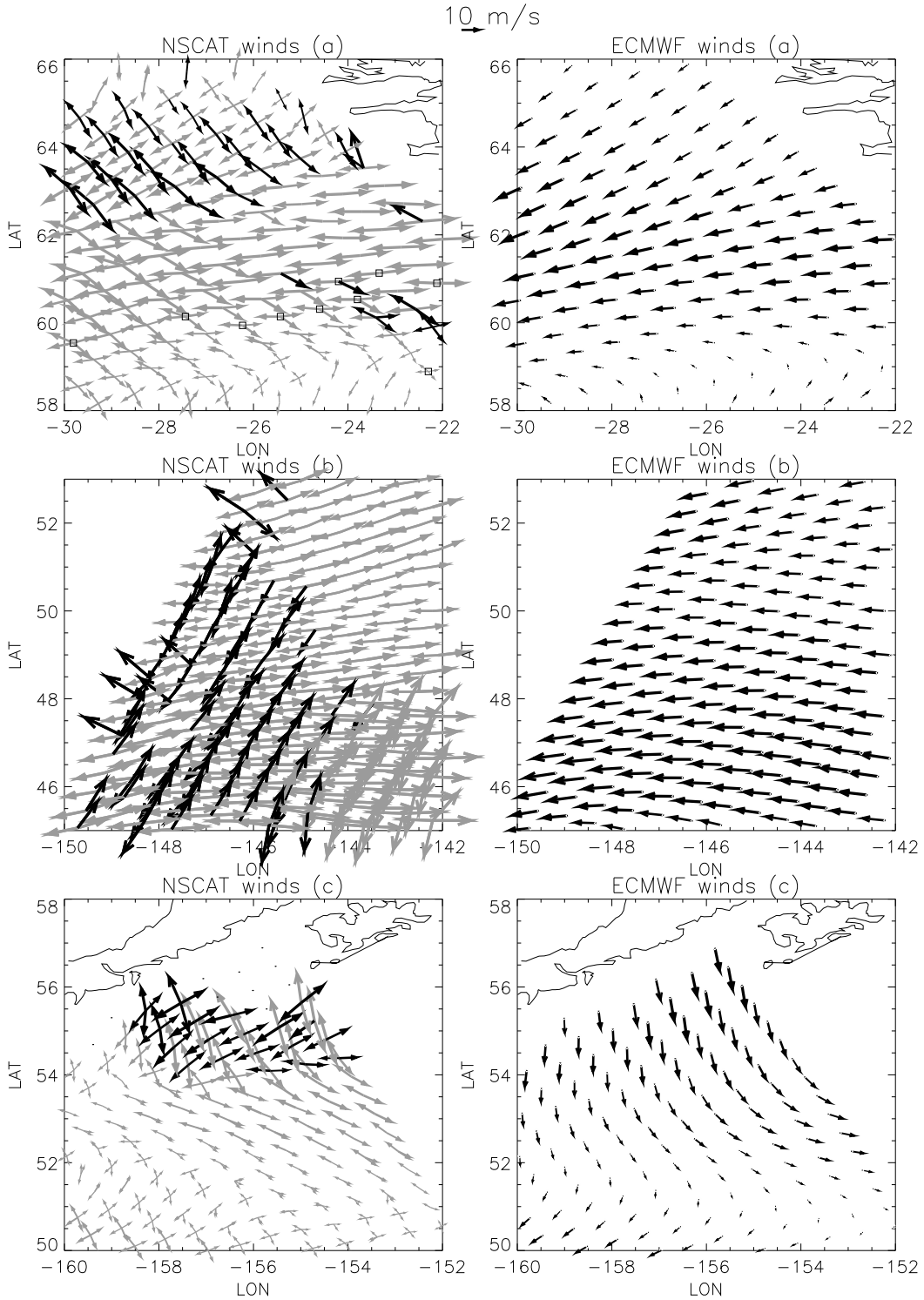

Figure 4 (a, b, c). Cases for illustration of how R_n assesses the information content of individual wind solutions. The left panels show all the solutions retrieved from NSCAT. In grey are the ones with $R_n < 2.0$ and in black those with $Rn \geq 2$ which are representative of our QC. The right panels show collocated ECMWF winds for each situation. Collocated SSM/I rain measurements are plotted as squares, the size of the square corresponding to the rain intensity. Three sizes are plotted for rain bellow 3(smallest), between 3 and 12 and above 12 mm/hr (biggest) respectively. The points represent locations for which a SSM/I collocation for NSCAT measurements could not be found. (Note that only one level of rain intensity (below 3 mm/hr) appears in figure 4a). Latitudes and longitudes are shown on the left and bottom respectively.

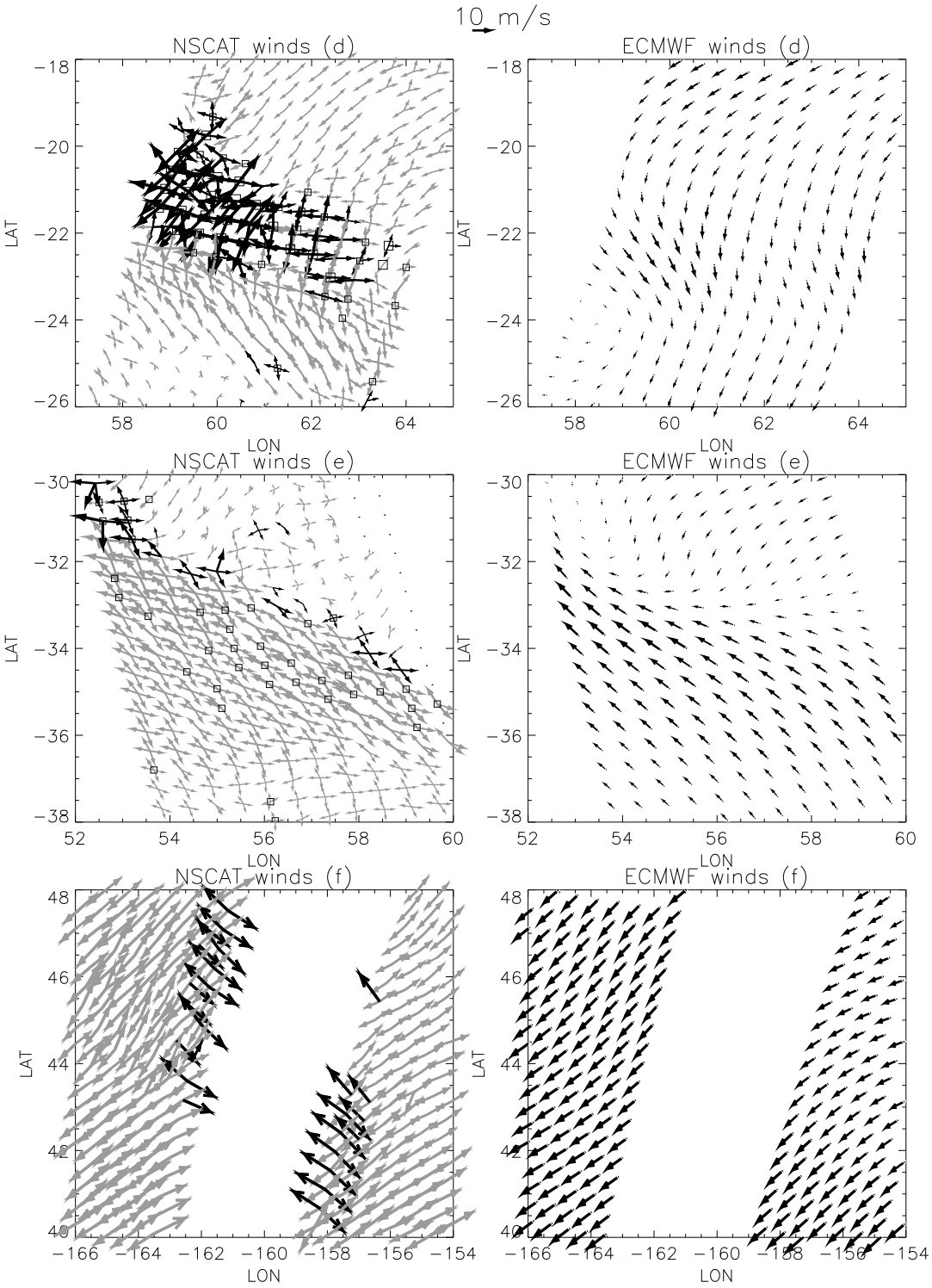

Figure 4 (d, e, f). As figure 4a. Note in this case that only one level of rain intensity (below 3 mm/hr) appears in figure 4e, while the three levels appear in figure 4d, the highest ones in the WVC towards the centre of the rain area).

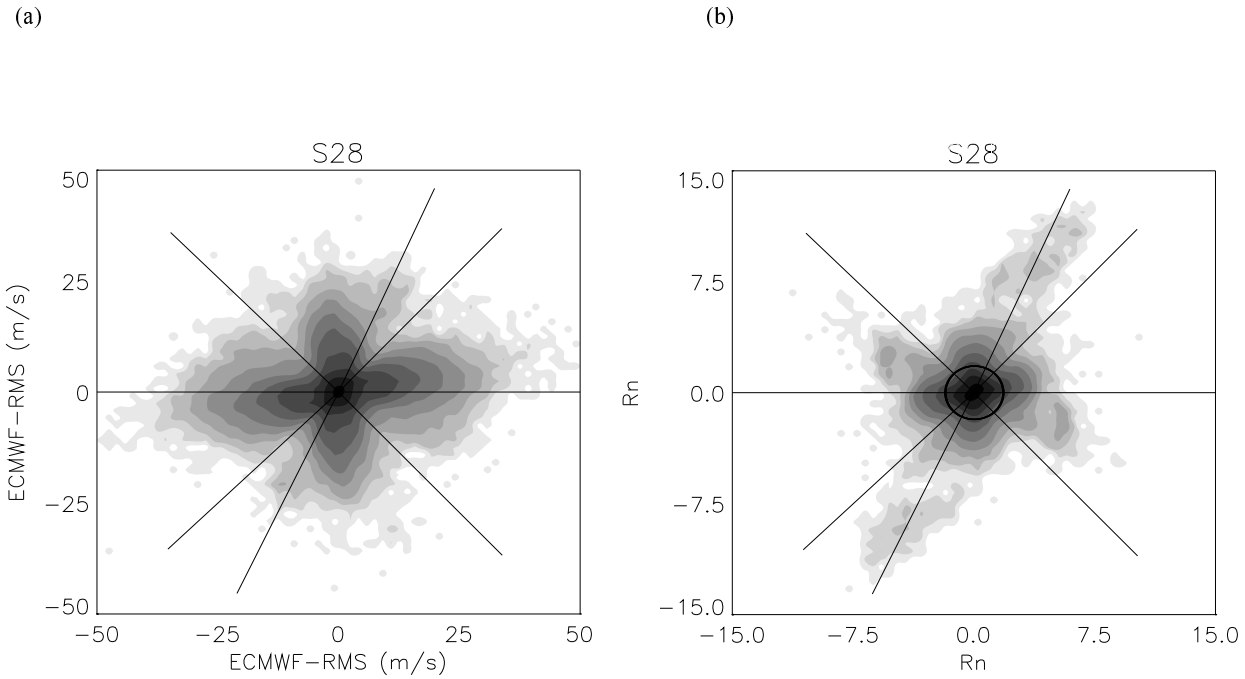

Figure 5. Polar plot representing the log-density scatter histograms of R_n and ECMWF-RMS values with respect to retrieved wind direction , relative to the satellite track (black line), for batch S28 of data. The darker areas show where the density of points is higher. In the white area no points were found. The grey scale is not linear, but logarithmic, in order to emphasise the distribution shape around the areas were higher values are found. The horizontal line represents the satellite direction, and the different antennae azimuths are plotted on top. The circle on the right plot corresponds to R_n=1.8.

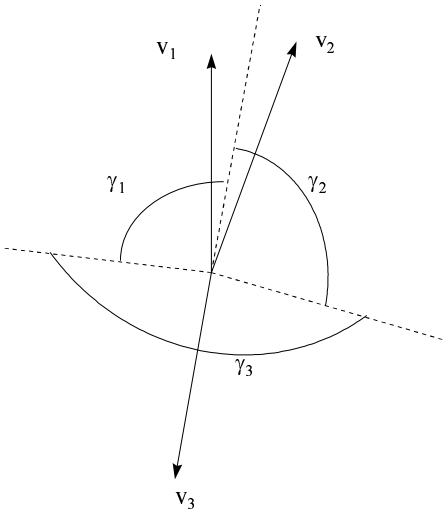

Figure 6: Given a number of ambiguous NSCAT solutions, v_i, an a-priori estimation of the probability of each of the ambiguous directions, p^d_i, can be given as proportional to the angle sector that every wind direction solution represents, γ_i.

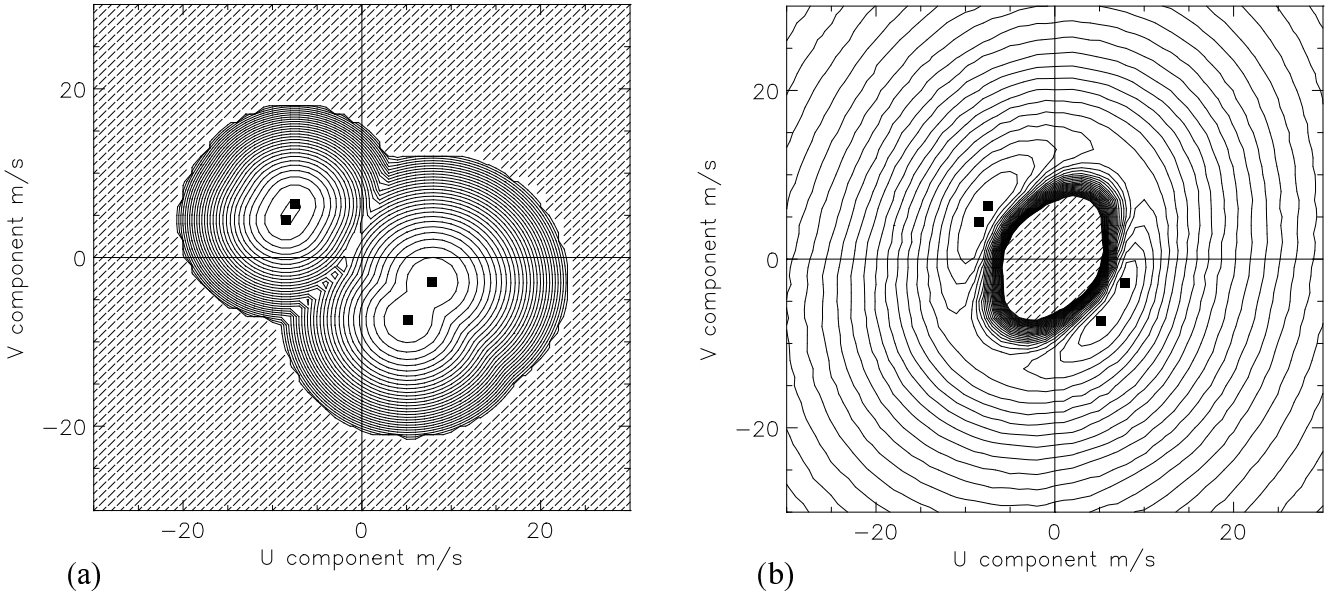

Figure 7. (a) Proposed cost function for the assimilation of NSCAT ambiguous winds in a 4D variational analysis. The cost function has been drawn using linearly increasing isolines for a typical symmetrical ambiguity situation. The (v,ϕ) solutions (squares), in (ms^{-1}, deg), are (9.8, 310.0), (9.6, 207.5), (9.0, 145.0) and (8.4, 110.0). Their corresponding R_n values are 0.27, 0.32, 0.67 and 0.8, respectively. The cost function relates to the probability of a wind vector in the wind domain for a given set of backscatter measurements. Away from the solutions, its value grows and the dashed area corresponds to a very high value, which is equivalent to a very small probability (large cost). (b) As a), but inversion residual (J) represented in the wind domain. It shows also minima at the wind solutions and for example extremely small probability for low wind speeds.